Weak values could reveal the hidden effects of quantum interactions

Miao Zhang*[1]

[1]*Department of Physics, Southwest Jiaotong University, Chengdu 610031, China*

(Dated: January 23, 2015)

Abstract

Due to the reduced probability of successful post-selection, the weak-value amplification seems to be unavailable for the parameter-estimation. Here, we show theoretically that, some effects due to the weak interactions present only in the properly post-selected sub-ensemble, however are canceled by themselves in the total ensemble. From this point of view, the post-selection induced weak value could be one of the feasible methods for measuring the weak interaction, since the standard measurement does not work. Additionally, we employ the system of trapped ions to simulate the weak measurement and calculate relevant results without the frequently-used weak interaction approximation.

* miaozhangphys@gmail.com

I. INTRODUCTION

The conception of quantum weak measurements was noticed by Aharonov, Albert, and Vaidman (AAV) in 1988 [1]. The weak measurements have two key features: the couplings between the quantum systems are sufficiently weak, and the relevant observable quantities (act as the pointers) are measured in the properly post-selected sub-ensemble. The outcome of weak measurements is the so-called weak value

$$A_w = \frac{\langle\psi_f|\hat{A}|\psi_i\rangle}{\langle\psi_f|\psi_i\rangle}\,, \tag{1}$$

where $|\psi_i\rangle$, $|\psi_f\rangle$, and $\hat{A}$ are the initial state, post-selected state, and the observable operator of the measured system, respectively. Comparing to the usual quantum measurement $A = \langle\psi_i|\hat{A}|\psi_i\rangle$, the weak value A_w could generate some interesting results [1–5], as the post-selection $|\psi_f\rangle$ is induced.

Recently, the weak value has been employed to study the foundational questions of quantum mechanics, e.g., the Hardy's paradox [6], the Leggett-Garg inequality [7], the Heisenberg's uncertainty relation [8], the Cheshire Cat [9], and the superluminal velocities [10]. Much attentions are also paid on the practical applications of the weak value, e.g., detecting tiny values of a quantity [11]. Considering an observable quantity depends on $g|A_w|$ (with g being a small parameter) [12], then the weak value A_w can significantly change the pointer with $|\langle\psi_f|\psi_i\rangle| \to 0$, or say amplifying the weak signal of g [13–19]. However, serval recent papers claim this amplification offering no fundamental metrological advantage, due to the necessarily reduced probability of successful post-selection [20–23], i.e., $|\langle\psi_f|\psi_i\rangle|^2 \to 0$.

In this work, we recommend an useful weak value, which could reveal the hidden effects of the weak quantum interactions. Here the hidden effects mean that, the g-induced changes of some observable quantities can not be detected by the usual quantum measurement (with the total ensemble). However, these changes can be conditionally measured by the weak value technique. If these special observable quantities are the better ones for experimentally detecting, then the weak value technique could be considered as an effective candidate for measuring the small parameter g of weak interaction. Moreover, we prove the relevant results by a simple example which is calculated without the frequently-used weak interaction approximation, and employ the powerful experimental-system of trapped ions to simulate the weak measurements.

This work is organized as follows. In Sec. II, we show that the usual measurement can not detect some special effects of the weak quantum interactions. In Sec. III, we show the conditional measurements could reveal these hidden effects, and calculate an example without the usual

weak interaction approximation. In Sec. IV, we employ the trapped ions to simulate the weak measurement, and finally give a conclusion in Sec. V.

II. THE VANISHED EFFECTS OF ONE-ORDER g

We consider the standard von Neumann measurement Hamiltonian

$$\hat{H} = \hbar g_0 \hat{A}\hat{P}\,. \tag{2}$$

Where, $\hbar$ is the Planck constant divided by 2π, $\hat{A}$ and $\hat{P}$ are respectively the operators of the qubit and the pointer (with the coupling frequency g_0 between them). After the above interaction, the final state of the total system can be formally written as

$$|\psi_f\rangle = e^{-ig\hat{A}\hat{P}}|S_0\rangle|\phi_0\rangle\,. \tag{3}$$

Where, $g = g_0 t$ (with the interaction duration t) describes the coupling strength between the pointer and the qubit, $|S_0\rangle$ and $|\phi_0\rangle$ are respectively the initial states of the qubit and the pointer. Considering the interaction is sufficiently weak, i.e., $g \to 0$, then the final state (3) can be approximately written as

$$|\psi_f\rangle \approx |S_0\rangle|\phi_0\rangle - ig\hat{A}\hat{P}|S_0\rangle|\phi_0\rangle\,. \tag{4}$$

by neglecting the high order of $O(g^2)$.

Directly, the probability of finding the pointer state $|x\rangle$ reads

$$\begin{aligned} I &= |\langle x|\psi_f\rangle|^2 \\ &\approx |\langle x|\phi_0\rangle|^2 - ig\left(\langle\phi_0|x\rangle\langle x|\hat{P}|\phi_0\rangle\langle S_0|\hat{A}|S_0\rangle - \text{c.c}\right) \\ &= I_0\left[1 - ig(P_w\langle S_0|\hat{A}|S_0\rangle - \text{c.c})\right] \\ &= I_0\left[1 + 2g\text{Im}(P_w\langle S_0|\hat{A}|S_0\rangle)\right] \end{aligned} \tag{5}$$

with $I_0 = |\langle x|\phi_0\rangle|^2$ and

$$P_w = \frac{\langle x|\hat{P}|\phi_0\rangle}{\langle x|\phi_0\rangle}\,. \tag{6}$$

Above, c.c is the conjugate complex number of the first term in the bracket, and the high order of $O(g^2)$ has been neglected again. This approximation shows that: when

$$P_w\langle S_0|\hat{A}|S_0\rangle = \text{Real}\,, \tag{7}$$

there is no effect due to the one-order g. Thus, we say that: the observable I is insensitive to the parameter g, and the weak-value amplification may be useful (when I is favorable for experimentally detecting).

Worth of note that, if $|x\rangle$ is the state of atoms at position x, the observable I can be regarded as the *"lightness"* of atoms beam. This is similar to the light intensity, which is proportional to $|\vec{E}(x)|^2$ of the Maxwell field $\vec{E}(x)$. Specially, we consider the two-level transition operator $\hat{A} = \hat{\sigma}_x = |e\rangle\langle g| + |g\rangle\langle e|$ and the initial state $|S_0\rangle = \alpha|g\rangle + \beta|e\rangle$ of the qubit. Here, α and β are the normalized coefficients of the two orthogonal states $|g\rangle$ and $|e\rangle$. When $P_w = \text{Real}$, the Eq. (5) can be rewritten as

$$\begin{aligned} I &= I_0\left[1 - igP_w\left(\alpha^*\beta + \beta^*\alpha - \text{c.c}\right)\right] \\ &= I_0\left[1 + 2gP_w\text{Im}(\alpha^*\beta) - 2gP_w\text{Im}(\alpha^*\beta)\right] \\ &= I_0 + I_g - I_g \\ &= I_0 \end{aligned} \tag{8}$$

with $I_g = 2gP_w\text{Im}(\alpha^*\beta)I_0$. This result shows that, under the condition of (7), the g-induced effects are accurately canceled by themselves.

III. THE WEAK MEASUREMENTS

With the post-selected state $|S_f\rangle$ of the qubit, the probability of finding the pointer state $|x\rangle$ reads:

$$\begin{aligned} I_s &= |\langle x|\langle S_f|\psi_f\rangle|^2 \\ &\approx \left|\langle S_f|S_0\rangle\langle x|\phi_0\rangle - ig\langle S_f|\hat{A}|S_0\rangle\langle x|\hat{P}|\phi_0\rangle\right|^2 \\ &\approx I_0 \times |\langle S_f|S_0\rangle|^2 \times [1 - igP_w(A_w - \text{c.c})] \\ &= I_0 \times |\langle S_f|S_0\rangle|^2 \times [1 + 2gP_w\text{Im}(A_w)] \end{aligned} \tag{9}$$

with the weak value

$$A_w = \frac{\langle S_f|\hat{A}|S_0\rangle}{\langle S_f|S_0\rangle}\,. \tag{10}$$

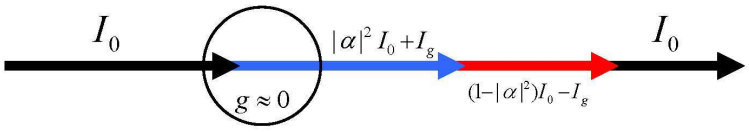

FIG. 1: (Color online) Sketch for the observable $I_0 = |\langle x|\phi_0\rangle|^2$ affected by the one-order g. Under the situation of Eq. (7), there is no effect of g with the usual measurement (the dark line). However, in the properly post-selected sub-ensemble (the red or blue line), the g-induced effect (i.e., I_g) appears.

The Eq. (9), with $A_w \neq$ Real, means that the effect due to the one-order g presents now in the post-selected sub-ensemble of $|S_f\rangle$. On the other hand, within the remaining sub-ensemble of $|S^f\rangle$, we have the similar result: the probability of finding $|x\rangle$ reads

$$I^s = I_0 \times \left|\langle S^f|S_0\rangle\right|^2 \times [1 + 2gP_w \mathrm{Im}(A^w)] \tag{11}$$

with the corresponding weak value

$$A^w = \frac{\langle S^f|\hat{A}|S_0\rangle}{\langle S^f|S_0\rangle}\,. \tag{12}$$

Considering $|S_f\rangle = |g\rangle$ and $|S^f\rangle = |e\rangle$, the Eq. (9) and (11) can be further written as

$$I_s = I_0 \times \left[|\alpha|^2 + 2gP_w \mathrm{Im}(\alpha^*\beta)\right]\,, \tag{13}$$

$$I^s = I_0 \times \left[|\beta|^2 - 2gP_w \mathrm{Im}(\alpha^*\beta)\right] \tag{14}$$

and then the total probability of finding the pointer state $|x\rangle$ reads

$$\begin{aligned} I_s + I^s &= I_0 \times [1 + 2gP_w \mathrm{Im}(\alpha^*\beta) - 2gP_w \mathrm{Im}(\alpha^*\beta)] \\ &= I_0 + I_g - I_g \\ &= I_0 \end{aligned} \tag{15}$$

This result is same to that of Eq. (8): the g-induced effects vanished from the usual measurement with the total ensemble. However, the Eq. (13) and (14) show that, the g-induced changing of observable I_0 presents magically in the properly post-selected sub-ensemble (see the dramatic Fig. 1). Moreover, it is easily to calculate the maximal $\mathrm{Im}(\alpha^*\beta) = 1/2$ (according to the normalized condition $|\alpha|^2 + |\beta|^2 = 1$). Thus, the Eq. (13) and (14) reduce further to $I_s = I_0 \times (\frac{1}{2} + gP_w)$ and $I^s = I_0 \times (\frac{1}{2} - gP_w)$, respectively.

We now calculate an example without the weak interaction approximation preformed in Eq. (4). Considering $\hat{P} = \hat{a}^\dagger \hat{a}$ and $\hat{A} = \hat{\sigma}_x$, the Hamiltonian (2) reads

$$\hat{H} = \hbar g_0 \hat{a}^\dagger \hat{a} \hat{\sigma}_x \,, \tag{16}$$

with $\hat{a}^\dagger$ and $\hat{a}$ being respectively the creation and annihilation operators in the Fock state presentation [24]. Without of generality, we write the initial state of the pointer as $|\phi_0\rangle = \sum_n c_n |n\rangle$, i.e., a superposed Fock state with the occupancy number $n \geq 0$ and the normalized coefficients $\sum_n |c_n|^2 = 1$. Consequently, the initial state of the total system reads

$$|\psi_0\rangle = |\phi_0\rangle(\alpha|g\rangle + \beta|e\rangle) = \sum_n c_n(\alpha|g\rangle + \beta|e\rangle)|n\rangle \tag{17}$$

and the final state reads

$$\begin{aligned} |\psi_f\rangle &= e^{-ig\hat{a}^\dagger \hat{a}\hat{\sigma}_x}|\psi_0\rangle = \textstyle\sum_n c_n(\alpha e^{-ig\hat{a}^\dagger \hat{a}\hat{\sigma}_x}|g\rangle|n\rangle + \beta e^{-ig\hat{a}^\dagger \hat{a}\hat{\sigma}_x}|e\rangle|n\rangle) \\ &= \textstyle\sum_n c_n \left(\alpha e^{-ign\hat{\sigma}_x}|g\rangle + \beta e^{-ign\hat{\sigma}_x}|e\rangle\right)|n\rangle \\ &= \textstyle\sum_n c_n \left\{\alpha[\cos(gn)|g\rangle - i\sin(gn)|e\rangle] + \beta[\cos(gn)|e\rangle - i\sin(gn)|g\rangle]\right\}|n\rangle \\ &= \textstyle\sum_n c_n \left(\eta_{gn}|g\rangle + \eta_{en}|e\rangle\right)|n\rangle \end{aligned} \tag{18}$$

with $\eta_{gn} = \alpha\cos(gn) - i\beta\sin(gn)$ and $\eta_{en} = \beta\cos(gn) - i\alpha\sin(gn)$. Immediately, we have

$$\begin{cases} |\eta_{gn}|^2 = |\alpha|^2\cos^2(gn) + |\beta|^2\sin^2(gn) - i\cos(gn)\sin(gn)(\beta\alpha^* - \alpha\beta^*) \\ |\eta_{en}|^2 = |\beta|^2\cos^2(gn) + |\alpha|^2\sin^2(gn) + i\cos(gn)\sin(gn)(\beta\alpha^* - \alpha\beta^*) \\ |\eta_{gn}|^2 + |\eta_{en}|^2 = 1 \end{cases} \tag{19}$$

and the following results.

(I) For the usual measurement of Fock state $|m\rangle$, we have

$$|\langle m|\psi_f\rangle|^2 = |c_m|^2 \left|(\eta_{gm}|g\rangle + \eta_{em}|e\rangle)\right|^2 = I_m \tag{20}$$

with $|c_m|^2 = I_m$.

(II) For the conditional measurement, we have

$$|\langle m|\langle g|\psi_f\rangle|^2 = I_m \left|\eta_{gm}\right|^2 \approx I_m[|\alpha|^2 + 2gm\mathrm{Im}(\alpha^*\beta)] \,, \tag{21}$$

$$|\langle m|\langle e|\psi_f\rangle|^2 = I_m \left|\eta_{em}\right|^2 \approx I_m[|\beta|^2 - 2gm\mathrm{Im}(\alpha^*\beta)] \,, \tag{22}$$

Here, we consider $gm \to 0$ and neglect the high order of $O(g^2)$. Thus, the results are same to that of Eq. (13) and (14) with $P_w = m$, and $|\langle m|\langle g|\psi_f\rangle|^2 + |\langle m|\langle e|\psi_f\rangle|^2 = |\langle m|\psi_f\rangle|^2 = I_m$.

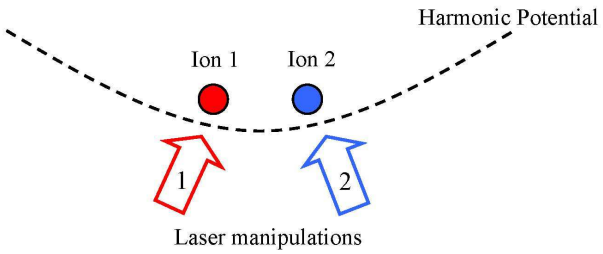

FIG. 2: (Color online) Sketch for the considered model to implement the weak measurement with trapped ions. Here, two ions are confined in a single harmonic potential and manipulated by the laser pulses. Two internal levels of ion 1 act as the quantum system (qubit), the center-of-mass (CM) motion of the two ions serves as the pointer. The laser 1 is applied to realize the desirable weak interaction (16) between the qubit and pointer, and the laser 2 couples the pointer (i.e., the CM mode) to the atomic levels of ion 2 for final readout (by the electron shelving method) [28].

IV. SIMULATING WEAK MEASUREMENT IN THE ION-TRAP

To simulate the above weak measurement, we consider two ions trapped in a linear Paul trap [25–28], as it showing dramatically in Fig. 2. The two internal atomic states of ion 1 is encoded as the qubit. By the so-called sideband excitation [26, 27], this qubit can be coupled to the center-of-mass (CM) motion of the two vibrational ions, and consequently the desirable Hamiltonian of (16) could be realized. The ion 2, manipulated by the lase beam 2, is used to experimentally measure the CM mode. Under the Lamb-Dicke approximation and the rotating wave approximation, the first-red-sideband excitation (generated by the laser pulse 1) is described by the well-known Hamiltonian [28]

$$\hat{H}_i = \hbar\Omega_0 \left(e^{i\delta t}\hat{a}\hat{\tau}_+ + e^{-i\delta t}\hat{a}^\dagger\hat{\tau}_-\right) . \tag{23}$$

Here, $\hat{a}^\dagger$ and $\hat{a}$ are respectively the boson creation and annihilation operators of the CM mode, $\hat{\tau}_+ = \mid\uparrow\rangle\langle\downarrow\mid$ and $\hat{\tau}_- = \mid\downarrow\rangle\langle\uparrow\mid$ are the two-level flip operators of ion 1 (with the internal states $\mid\downarrow\rangle$ and $\mid\uparrow\rangle$), and Ω_0 is the Rabi frequency of the sideband coupling, and δ is the relating detuning (decided by the frequencies of the applied laser beams). When $\delta = 0$, the Hamiltonian (23) describes a standard Jaynes-Cummings (JC) coupling between the internal and external states of trapped ions.

Under the large detuning: $\Omega \ll \delta$, the time-evolution operator of Hamiltonian (23) can be

approximately written as:

$$\hat{U}(t) = 1 + \left(\frac{-i}{\hbar}\right)\int_0^t \hat{H}_i(t_1)dt_1 + \left(\frac{-i}{\hbar}\right)^2 \int_0^t \hat{H}_i(t_1)\int_0^{t_1} \hat{H}_i(t_2)dt_2dt_1 + \cdots \approx e^{-\frac{i}{\hbar}\hat{H}_e t}\,, \tag{24}$$

with the effective Hamiltonian $\hat{H}_e = (\hbar\Omega_0^2/\delta)[\hat{a}^\dagger\hat{a}(|\uparrow\rangle\langle\uparrow| - |\downarrow\rangle\langle\downarrow|) + |\uparrow\rangle\langle\uparrow|]$ [29]. In the interaction picture defined by $\hat{U}_R = \exp(-ig_0t|\uparrow\rangle\langle\uparrow|)$, this Hamiltonian can be further written as

$$\hat{H}'_e = \hbar g_0 \hat{a}^\dagger\hat{a}\hat{\tau}_z \tag{25}$$

with $\hat{\tau}_z = |\uparrow\rangle\langle\uparrow| - |\downarrow\rangle\langle\downarrow|$ and $g_0 = \Omega_0^2/\delta$. We define $|e\rangle = \frac{1}{\sqrt{2}}(|\uparrow\rangle + |\downarrow\rangle)$ and $|g\rangle = \frac{1}{\sqrt{2}}(|\uparrow\rangle - |\downarrow\rangle)$ being the qubit of ion 1. These states satisfy the orthogonal condition $\langle e|g\rangle = 0$ and the normalized condition $\langle e|e\rangle = \langle g|g\rangle = 1$. As $\hat{\tau}_z|e\rangle = |g\rangle = \hat{\sigma}_x|e\rangle$ and $\hat{\tau}_z|g\rangle = |e\rangle = \hat{\sigma}_x|g\rangle$, the Hamiltonian (25) can be written as the desirable form $\hat{H} = \hbar g_0\hat{a}^\dagger\hat{a}\hat{\sigma}_x$ of Eq. (16) and consequently get the same results to (18).

Experimentally, the internal atomic states of the trapped ions can be well measured by serval methods such as the electron shelving technique [28]. This method can be briefly described as follows. Applying a strong laser resonantly drives the transition between the state $|\uparrow\rangle$ and an auxiliary atomic state $|\text{aux}\rangle$. If the ion is in state $|\uparrow\rangle$, the laser-induced resonance fluorescence can be quickly detected, whereas there is no signal as the transition $|\downarrow\rangle \Leftrightarrow |\text{aux}\rangle$ is large detuning. Here, the post-selection (i.e., the detection of state $|e\rangle$ or $|g\rangle$) needs additional operations, since these states are the superposition ones of $|\uparrow\rangle$ and $|\downarrow\rangle$. We apply a single-qubit operation to the ion 1, i.e., $\hat{U}_s = \exp(-i\hat{H}_s t/\hbar)$ with the Hamiltonian $\hat{H}_s = \hbar\Omega_s(e^{-i\theta}\hat{\sigma}_+ + e^{i\theta}\hat{\sigma}_-)$. By setting the parameters $\Omega_s t = \pi/4$ and $\theta = -\pi/2$, we have $\hat{U}_s|e\rangle = |\uparrow\rangle$ and $\hat{U}_s|g\rangle = -|\downarrow\rangle$. Consequently, we have

$$|\psi'_f\rangle = \hat{U}_s|\psi_f\rangle = \sum_n c_n\left(\eta_{gn}\hat{U}_s|g\rangle + \eta_{en}\hat{U}_s|e\rangle\right)|n\rangle = \sum_n c_n\left(\eta_{en}|\uparrow\rangle - \eta_{gn}|\downarrow\rangle\right)|n\rangle \tag{26}$$

and the same results to (20) $\sim$ (22), i.e.,

$$\begin{cases} \left|\langle m|\psi'_f\rangle\right|^2 = I_m\,, \\ \left|\langle m|\langle\downarrow|\psi'_f\rangle\right|^2 \approx I_m[|\alpha|^2 + 2gm\text{Im}(\alpha^*\beta)]\,, \\ \left|\langle m|\langle\uparrow|\psi'_f\rangle\right|^2 \approx I_m[|\beta|^2 - 2gm\text{Im}(\alpha^*\beta)]\,. \end{cases} \tag{27}$$

As that demonstrated in many experiments, the external motional states of trapped ions can be mapped to their internal states by the laser manipulations [26–28], and measured consequently by the electron shelving technique. For simplicity, we suppose that the CM mode is prepared

initially in the superposition state $|\phi_0\rangle = \sum_{n=0}^{1} c_n|n\rangle = c_0|0\rangle + c_1|1\rangle$ (with the normalized coefficients $|c_0|^2 + |c_1|^2 = 1$), and the internal state of ion 2 is initially in $|\downarrow_r\rangle$. We apply a first-red-sideband laser pulse to implement the operation $\hat{U}_r = \exp(-i\hat{H}_r t/\hbar)$ on ion 2. Here, $\hat{H}_r = \hbar\Omega_r\left(\hat{a}\hat{\tau}_{2+} + \hat{a}^\dagger\hat{\tau}_{2-}\right)$ is the JC coupling between the CM mode and the internal states of ion 2, with the two-level flip operators $\hat{\tau}_{2+} = |\uparrow_r\rangle\langle\downarrow_r|$ and $\hat{\tau}_{2-} = |\downarrow_r\rangle\langle\uparrow_r|$. When $\Omega_r t = \pi/2$, this operation generates the logic: $|0\rangle|\downarrow_r\rangle \rightarrow |0\rangle|\downarrow_r\rangle$, $|1\rangle|\downarrow_r\rangle \rightarrow (-i)|0\rangle|\uparrow_r\rangle$. Consequently, we have

$$\begin{cases} \left|\langle\uparrow_r|\psi_f''\rangle\right|^2 = \left|\langle m|\psi_f'\rangle\right|^2 = I_m\,, \\ \left|\langle\uparrow_r|\langle\downarrow|\psi_f''\rangle\right|^2 = \left|\langle m|\langle\downarrow|\psi_f'\rangle\right|^2 \approx I_m[|\alpha|^2 + 2gm\mathrm{Im}(\alpha^*\beta)]\,, \\ \left|\langle\uparrow_r|\langle\uparrow|\psi_f''\rangle\right|^2 = \left|\langle m|\langle\uparrow|\psi_f'\rangle\right|^2 \approx I_m[|\beta|^2 - 2gm\mathrm{Im}(\alpha^*\beta)]\,. \end{cases} \tag{28}$$

with $|\psi_f''\rangle = \hat{U}_r|\psi_f'\rangle|\downarrow_r\rangle$ and $m = 1$. These results are same to that of Eq. (27). Worth of note that, the above operations (i.e., $\hat{U}_s$, $\hat{U}_r$, and the preparation and readout of the initial and final states) are that frequently used in the system of laser-manipulated trapped ions. Thus, the above simulation of weak measurements could be experimentally feasible. Indeed, the quantum entanglement with eight ions has been successfully demonstrated (need more operations) in this powerful experimental platform [30].

V. CONCLUSION

In this study, we present a very simple version to explain the usefulness of weak values. We showed that the weak values work well under the certain conditions, e.g., Eq. (7). With this equation, some effects of the weak interactions present only in the properly post-selected sub-ensemble, however are canceled by themselves in the total ensemble. From this point of view, the weak value can be regarded as one of the effective methods for measuring the weak interaction, as the usual measurement does not work. We presented an example to exactly calculate the relevant results. These results prove that the frequently-used weak interaction approximation is effective indeed. Additionally, we showed that the famous experimental-system of trapped ions could also be utilized to simulate the weak measurements. Finally, we hope this paper could help understanding the weak values and moving the relevant researches forward.

Acknowledgements: This work was supported by the National Natural Science Foundation of China Grants No. 11204249.

[1] Y. Aharonov, D. Z. Albert, and L. Vaidman, Phys. Rev. Lett. **60**, 1351 (1988).

[2] J. S. Lundeen, B. Sutherland, A. Patel, C. Stewart, and C. Bamber, Nature **474**, 188 (2011).

[3] S. Kocsis, B. Braverman, S. Ravets, M. J. Stevens, R. P. Mirin, L. K. Shalm, and A. M. Steinberg, Science **332**, 1170 (2011).

[4] O. Hosten and P. Kwiat, Science **319**, 787 (2008).

[5] M. F. Pusey, Phys. Rev. Lett. **113**, 200401 (2014).

[6] J. S. Lundeen and A. M. Steinberg, Phys. Rev. Lett. **102**, 020404 (2009).

[7] J. Dressel, C. J. Broadbent, J. C. Howell, and A. N. Jordan, Phys. Rev. Lett. **106**, 040402 (2011).

[8] L. A. Rozema, A. Darabi, D. H. Mahler, A. Hayat, Y. Soudagar, and A. M. Steinberg, Phys. Rev. Lett. **109**, 100404 (2012).

[9] T. Denkmayr, H. Geppert, S. Sponar, H. Lemmel, A. Matzkin, J. Tollaksen, and Y. Hasegawa, Nature Communications **5**, 4492 (2014).

[10] N. Brunner, V. Scarani, M. Wegmüller, M. Legré, and N. Gisin, Phys. Rev. Lett. **93**, 203902 (2004).

[11] J. Dressel, M. Malik, F. M. Miatto, A. N. Jordan, and R. W. Boyd, Rev. Mod. Phys. **86**, 307 (2014).

[12] R. Jozsa, Phys. Rev. A **76**, 044103 (2007).

[13] P. B. Dixon, D. J. Starling, A. N. Jordan, and J. C. Howel, Phys. Rev. Lett. **102**, 173601 (2009).

[14] O. S. Magaña-Loaiza, M. Mirhosseini, B. Rodenburg, and R. W. Boyd, Phys. Rev. Lett. **112**, 200401 (2014).

[15] S. Pang, J. Dressel, and T. A. Brun, Phys. Rev. Lett. **113**, 030401 (2014).

[16] A. Feizpour, X. Xing, and A. M. Steinberg, Phys. Rev. Lett. **107**, 133603 (2011).

[17] Y. Susa, Y. Shikano, and A. Hosoya, Phys. Rev. A **85**, 052110 (2012).

[18] G. I. Viza, J. M. Rincón, G. B. Alves, A. N. Jordan, and J. C. Howell, arXiv: 1410.8461v1.

[19] J. P. Torres and L. J. Salazar-Serrano, arXiv: 1408.1919v1.

[20] X. Zhu, Y. Zhang, S. Pang, C. Qiao, Q. Liu, and S. Wu, Phys. Rev. A **84**, 052111 (2011).

[21] C. Ferrie and J. Combes, Phys. Rev. Lett. **112**, 040406 (2014).

[22] G. C. Knee and E. M. Gauger, Phys. Rev. X **4**, 011032 (2014).

[23] G. C. Knee, J. Combes, C. Ferrie, and E. M. Gauger, arXiv: 1410.6252v1.

[24] C. Simon and E. S. Polzik, Phys. Rev. A **83**, 040101 (2011).

[25] J. I. Cirac and P. Zoller, Phys. Rev. Lett. **74**, 4091 (1995).

[26] C. Monroe, D. M. Meekhof, B. E. King, W. M. Itano, and D. J. Wineland, Phys. Rev. Lett. **75**, 4717 (1995).

[27] D. M. Meekhof, C. Monroe, B. E. King, W. M. Itano, and D. J. Wineland, Phys. Rev. Lett. **76**, 1796 (1995).

[28] D. Leibfried, R. Blatt, C. Monroe, and D. Wineland, Rev. Mod. Phys. **75**, 281 (2003).

[29] M. Zhang and S. Y. Zhu, arXiv:1410.7152v1.

[30] H. Häffner, W. Hänsel, C. F. Roos, J. Benhelm, D. Chek-al-kar, M. Chwalla, T. Körber, U. D. Rapol, M. Riebe, P. O. Schmidt, C. Becher, O. Gühne, W. Dür, and R. Blatt, Nature **438**, 643 (2005).